# AC loss calculation in high-temperature superconductor wires and windings with analytical and numerical models: influence of $J_c(B)$ dependence

# AC loss calculation in high-temperature superconductor wires and windings with analytical and numerical models: influence of $J_c(B)$ dependence

**Francesco Grilli**[1], **Sunny Abraham**[1], **Roberto Brambilla**[2]

[1]Institute for Technical Physics, Karlsruhe Institute of Technology, Karlsruhe, Germany
[2]Ricerca Sistema Energetico, Milan, Italy (formerly)

E-mail: francesco.grilli@kit.edu

**Abstract.** Too high loss levels can severely limit the efficiency and the safe operation of several high-temperature superconductor (HTS) AC applications. A reliable estimation of AC losses, which includes the observed field-dependence of the superconductor's critical current density on the magnetic field, is therefore paramount. In this contribution, we use numerical simulations to evaluate the AC losses of HTS coated conductors in a variety of working scenarios: individual wires carrying AC transport current and/or subjected to AC magnetic fields, and wire assemblies like stacks and arrays carrying AC transport current. Numerical results are compared to the corresponding analytical models and to experimental results. This work presents some general guidelines regarding the extent to which the dependence of the critical current density $J_c$ on the magnetic flux density $B$ modifies the AC loss characteristics with respect to a constant-$J_c$ model based on the superconductor's self-field critical current.

## 1. Introduction

In recent years, numerous high-temperature superconductor (HTS) applications have been developed. As a consequence, the demand for numerical tools able to quickly estimate the energy dissipation caused by time-varying magnetic fields has also increased. Among those tools, analytical models are particularly sought-after, because, by using relatively simple mathematical expressions, they provide a quasi-instantaneous evaluation of the energy losses. Although these analytical models cannot handle the same degree of complexity as numerical models [1], they are the preferred solution when a precise evaluation of the losses is not necessary, and one just needs to quickly establish general trends. In general, analytical models assume a constant critical current density $J_c$ for the superconductor. However, $J_c$ depends on the magnetic flux density $B$, and the dependence can also take quite complex forms.

In this contribution, we evaluate the difference between using constant-$J_c$ and $J_c(B)$ models for calculating AC losses in different scenarios: individual HTS wires carrying AC transport current, subjected to AC magnetic field, or both; we also explore the case of interacting tapes in the form of horizontal arrays and vertical stacks. The vertical stack resembles the arrangement of superconducting wires in racetrack or pancake coils, whereas the horizontal array that of wires in solenoids. We compare analytical results with numerical ones based on a well-established finite-element method approach. Additionally, we present experimental results from the literature and assess the level of agreement between experimental and calculated data.

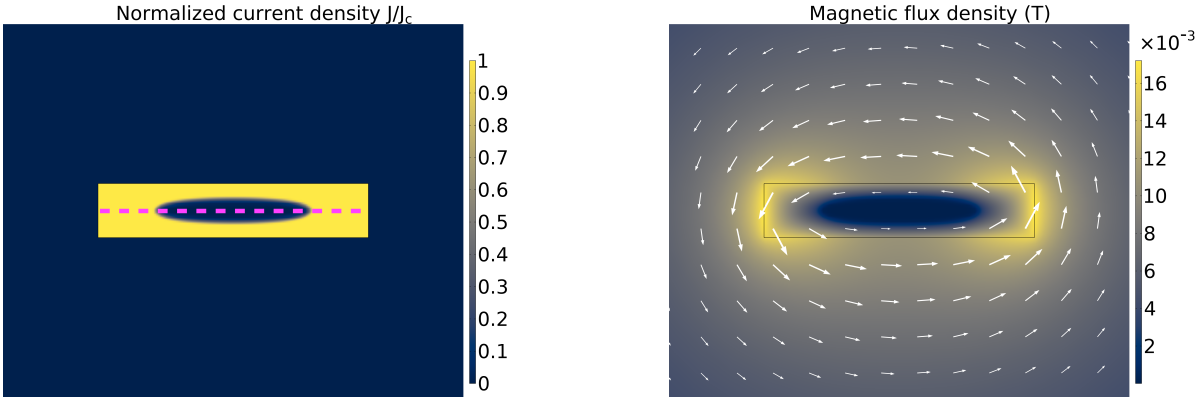


(a) (b)

Figure 1: Distributions of normalized current density (a) and magnetic flux density (b) in a superconducting wire of rectangular cross section carrying 80 % of the critical current calculated with the critical state model [4, 5]. The distributions are taken at the peak of the sinusoidal transport current. The dashed line marks the center of the rectangle (see text).

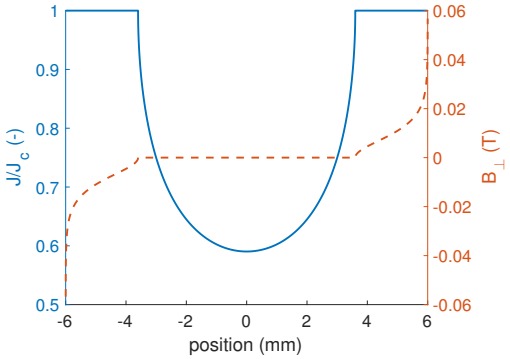


Figure 2: Distributions of normalized current density (a) and magnetic flux density (b) in an infinitely thin strip carrying 80 % of the critical current calculated with the critical state model [6, 7]. The distributions are taken at the peak of the sinusoidal transport current and calculated with formulas 2.4 and 2.6 of [6]

## 2. Analytical and numerical models

### *2.1. Analytical models for AC loss calculation*

The analytical models for calculating AC losses in superconductors are mostly based on the critical state model developed by Bean in the 1960s [2, 3], according to which currents of magnitude $J_c$ are produced by a non-zero electric field regardless of its magnitude and rate of variation.

The superconducting layer of HTS coated conductors has an extremely large width-to-thickness ratio. From the point of view of analytical models, this means that the superconducting layer can be approximated as infinitely thin and, under the assumption that nothing changes along the wire's length, treated as a 1D object. The magnetic field and current distributions are calculated only along the superconductor's width and present no variation along the thickness.

The shapes of the current density and magnetic field distributions in an infinitely thin superconductor can be understood by considering that geometry as a limit of a finite rectangular one when the thickness approaches zero. Figures 1a and 1b show the distributions of normalized current density and magnetic flux density in a superconducting wire of rectangular cross section carrying 80 % of the critical current, based on the critical state model [4, 5]. The distributions are taken at the peak of the sinusoidal transport current. The current density is equal to $J_c$ except in the central field-free region, where it is zero. As the rectangle becomes infinitely thin,

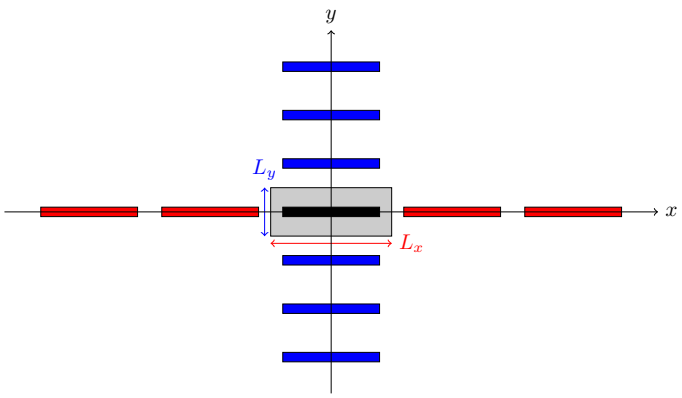


Figure 3: Schematic representation of an infinite vertical stack (blue) and an infinite horizontal array (red) of HTS wires. The grey rectangle represents the size ($L_x$ or $L_y$) of one dimension of the periodic cell in the two cases.

we can take the current distribution along the dashed line in figure 1a as the average of $J$ along the rectangle's thickness. This results in a critical current equal to $J_c$ in the two regions near the edges and in a subcritical value in the central field-free region. The horizontal field component (parallel to the wide face of the HTS wire) is always zero along the dashed line. This means that, in the infinitely thin strip limit, such component is not defined inside the superconductor; outside the superconductor, the horizontal field component switches between negative and positive values on the two sides of the strip.

With the infinitely-thin strip approximation, relatively simple formulas exist for computing AC losses [6, 7, 8]. In this work, we investigate the following cases:∗

- Individual wire carrying an AC current of amplitude $I_0$

$$Q_t = \frac{\mu_0 I_c^2}{\pi}\left[(1-i_0)\ln(1-i_0)+(1+i_0)\ln(1+i_0)-i_0^2\right] \tag{1}$$

- Individual wire subjected to an AC field of amplitude $B_0 = \mu_0 H_0$

$$Q_m = 4\mu_0 w^2 \tilde{J}_c H_0 g(H_0/H_c) \tag{2}$$

- Infinite horizontal array of wires carrying an AC current of amplitude $I_0$

$$Q_a = \frac{\mu_0 I_c^2}{\pi} i_0^2 \int_0^1 (1-2s)\ln\left[1-\frac{\tan^2(\pi i_0 s w/L_x)}{\tan^2(\pi w/L_x)}\right] \mathrm{d}s \tag{3}$$

- Infinite vertical stack of wires carrying an AC current of amplitude $I_0$

$$Q_s = \frac{\mu_0 I_c^2}{\pi} i_0^2 \int_0^1 (1-2s)\ln\left[\frac{\cosh^2(\pi w/L_y)}{\cosh^2(\pi i_0 s w/L_y)}-1\right] \mathrm{d}s. \tag{4}$$

In the equations above, $I_c$ is the wire's critical current, $i_0 = I_0/I_c$ is the fraction of $I_c$ that is transported by the wire, $w$ is the wire's half width, $\tilde{J}_c = I_c/w$ is the *sheet* critical current density, $H_c = \tilde{J}_c/\pi$ is a characteristic magnetic field, $g(x) = (2/x)\ln\cosh x - \tanh x$, and $L_x$ and $L_y$ are the periodic cells for an array and a stack, respectively (see figure 3).

All the formulas listed above assume a constant $J_c$. In this contribution, we compare the analytical results with those obtained with a numerical model, where the $J_c(B)$ dependence can be included.

∗For the simulation of an HTS wire, we consider only the superconducting layer. As shown in [9], the metallic layer do not contribute significantly for the situations analyzed here. As a consequence, in the rest of the paper, we use the words "superconductor" and "wire" interchangeably.

*2.2. Choice of $J_c(B)$*

In this work, we considered a superconductor 12 mm wide, 1 µm thick, and with a self-field critical current of 360 A at 77 K. For the constant-$J_c$ models, $J_c = 3 \times 10^{10}\,\mathrm{A\,m^{-2}}$. For the $J_c(B)$ models, we used the following expression:

$$J_c(B) = \frac{J_{c0}}{(1 + B_\perp/B_0)^\alpha}, \tag{5}$$

where $B_0 = 10\,\mathrm{mT}$, $\alpha = 0.5$, and $B_\perp$ is the magnitude of the magnetic flux density component perpendicular to the wire's surface. We chose $J_{c0} = 4.84 \times 10^{10}\,\mathrm{A\,m^{-2}}$ so that the self-field critical current of the wire – calculated with the 2D method described in [10] – is 360 A.

*2.3. Numerical model for AC loss calculation*

As a numerical model, we chose the finite-element solution of Maxwell's equations with the so-called $H$-formulation implemented in COMSOL Multiphysics [11, 12]. This is a widely adopted model for calculating AC losses [13] and, more generally, for investigating the electromagnetic behavior of HTS wires and applications [14]. The superconductor is simulated as a material with a nonlinear resistivity

$$\rho(J) = \frac{E_c}{J_c}\left(\frac{|\mathbf{J}|}{J_c}\right)^{n-1}, \tag{6}$$

where $E_c = 1 \times 10^{-4}\,\mathrm{V\,m^{-1}}$, $n = 35$, and $J_c$ is either constant or dependent on the magnetic field. The superconductor is discretized with a $250 \times 1$ mesh.

The simulation of horizontal arrays and vertical stacks of current-carrying wires can be performed by simulating only one periodic cell with a wire at its center (figure 3, grey rectangle). One side of the rectangle has the length of the periodic cell (for example $L_y$ in the case of a vertical stack); the other side is made very long. Appropriate periodicity conditions need to be set in COMSOL Multiphysics's *mfh* module to guarantee the continuity of the magnetic field in the periodical direction.

## 3. Results

The $J_c(B)$ dependence changes the local transport capacity of the superconductor. In general, this results in different current density distributions from those obtained with constant $J_c$. An example for the case of transport current equal to $0.8I_c$ is shown in figure 4. The maximum of the (self-generated) magnetic field is at the superconductor's edges (figure 2). With a $J_c(B)$ dependence like equation (5), near the edges the critical current density is much lower than $J_{c0}$. As a consequence, the maximum of the current density is located inside the tape (figure 4a).

Figure 5a displays the transport losses calculated with the constant-$J_c$ and $J_c(B)$ models as a function of different transport currents. The cyclic losses are computed by averaging the power dissipation on the second half of the first simulated AC cycle, as

$$Q = \frac{2}{T}\int_{T/2}^{T}\int_{\Omega} \rho J^2 \,\mathrm{d}\Omega\,\mathrm{d}t, \tag{7}$$

where $T$ is the period of the AC cycle (20 ms for the 50 Hz frequency considered in this work) and $\Omega$ is the superconductor's domain.

The losses computed with the two models are similar, because despite the differences in the $J$ distributions (figure 4a), the dissipative regions where $J/J_c \geq 1$ are of similar size (figure 4b). The numerical results are also in good agreement with the analytical ones given by formula (1). Reported in the figure are also experimental results from different sources [9, 15, 16, 17]. Since

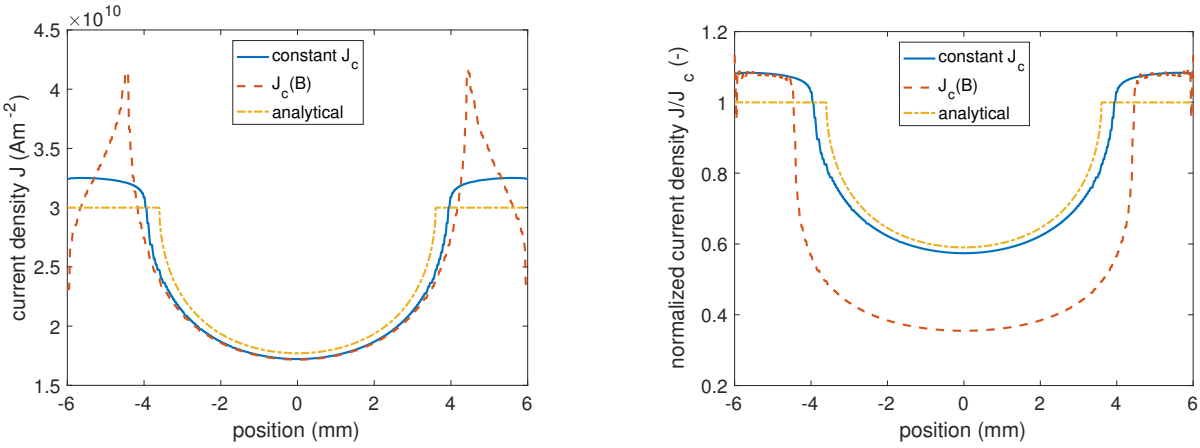


(a) (b)

Figure 4: Distributions of current density (a) and normalized current density (b) along the width of a superconducting strip carrying 80 % of the critical current, calculated with constant and magnetic-field-dependent $J_c$. The distributions are taken at the peak of the sinusoidal transport current. The analytical curves are the same as that of figure 2.

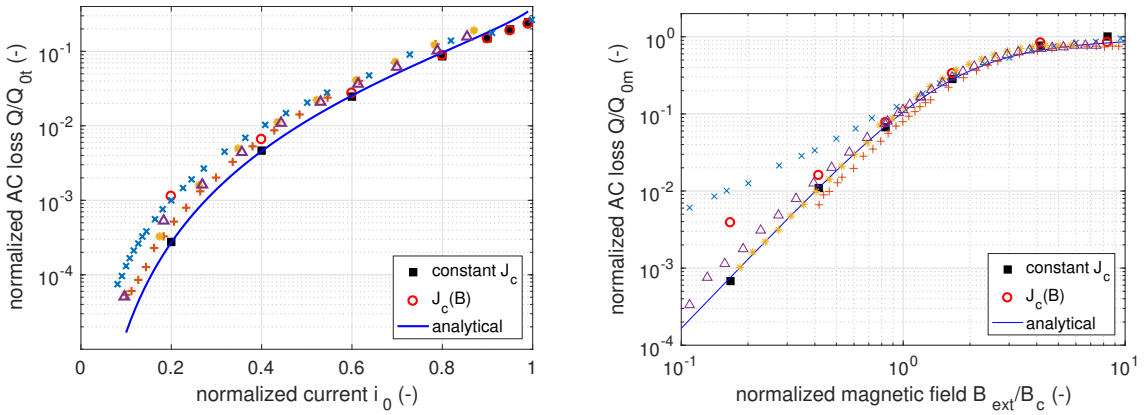


(a) (b)

Figure 5: Comparison of AC losses of an individual superconductor, calculated with constant-$J_c$ (solid squares) and $J_c(B)$ (empty circles): (a) Transport losses: analytical results from (1), experimental data from [9, 15, 16, 17]; (b) Magnetization losses: analytical results from (2), experimental data from [15, 16, 18, 19].

the samples are characterized by different critical currents, the transport current and the AC losses are normalized by the critical current $I_c$ and by the factor $Q_{0t} = \mu_0 I_c^2/\pi$, respectively – see equation (1). In general the experimental results are in good agreement with the models. The discrepancy observed at low current is usually ascribed to a degradation of $J_c$ near the edges of the wire [20].

Similar conclusions apply to the case of the magnetization losses (figure 5b) caused by an AC magnetic field applied perpendicular to the superconductor's wide face. In this case, the applied field $B_{ext}$ is normalized by the characteristic field $B_c = \mu_0 H_c = 12\,\mathrm{mT}$ and the losses by the factor $Q_{0m} = 4\mu_0 w^2 \tilde{J}_c H_0$ – see equation (2). Reported in the figure are also experimental results from different sources [15, 16, 18, 19]. Similar to the case of transport current, the experimental

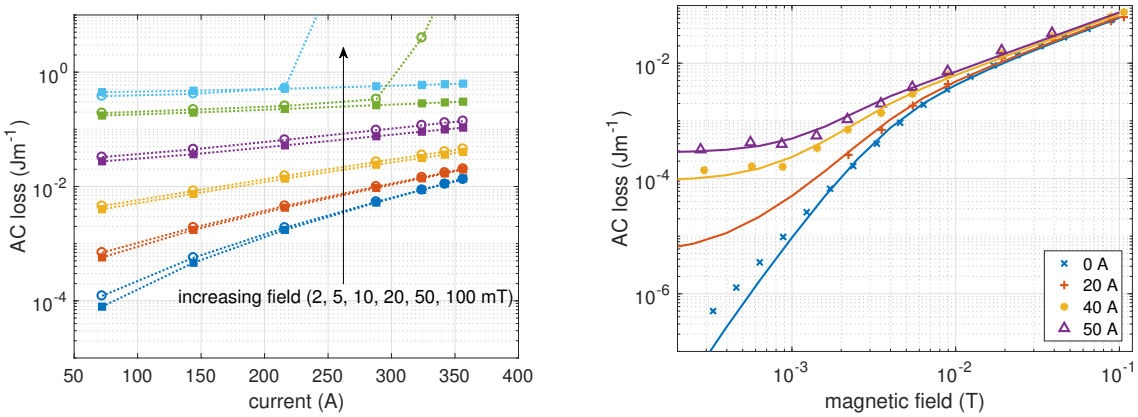


Figure 6: Total losses due to the simultaneous presence of AC transport current and AC background field: (a) Comparison of results obtained with constant-$J_c$ and $J_c(B)$ models for fields of 2, 5, 10, 20, 50, 100 mT; (b) Comparison of calculations (constant-$J_c$) and experimental data from [21].

values are higher than those predicted by the models, especially for one sample. Again, this is ascribed to the degradation of $J_c$ near the edges [15]. This discrepancy has little practical relevance, because it appears at very low values of transport current and applied field, which are not those at which the superconducting wire usually operates in real applications.

Figure 6a shows the total losses in a single superconductor carrying an AC transport current while subjected to an in-phase AC background field of increasing amplitude. For applied fields up to 20 mT (purple data points), the constant-$J_c$ and $J_c(B)$ models give similar AC loss estimations. Starting from the 50 mT curve (green data points), one can observe a sudden increase of the losses with the $J_c(B)$: this is because the external field strongly reduces $J_c$ and a transport current of 288 A is greater than the effective $I_c$ of the wire. At higher fields (100 mT, light blue data points), the sudden increase of the losses occurs at lower current. In figure 6a, one can also observe that the slope of the loss curve decreases as the magnetic field increases: this is because the influence of the transport current decreases as the field becomes larger.

Figure 6b shows a comparison between calculations and experimental data for the losses due to the simultaneous action of transport current and magnetic field [21]. The model reproduces the experiments well. At very low fields (less than 1 mT) the losses are mainly due to the current. Then, as the field increases, the influence of the applied field becomes more important, and eventually dominates.

Figure 7a shows the AC losses of a vertical stack for different separations $L_y$. The constant-$J_c$ results agree well with the values calculated with equation (4), given by the continuous lines. The values calculated with the $J_c(B)$ model are in general higher because of the self-field generated by the stack. They also present a steep increase at current values well below the wire's self-field critical current (360 A). Reducing the separation $L_y$ makes this change of slope of the curve occur at lower values of the current. This is due to the self-field generated by the superconductors in the stack, which reduces the transport capacity of the wire. This effect is visible by looking at the $J$ profiles of a given case, $L_y = 1$ mm, in figure 7b. As the transport current is increased (from 36 A to 288 A in steps of 36 A), the current penetrates toward the center. When $I_0 = 252$ A, the superconductor is already saturated with current.

Figure 8 presents the same type of results as figure 7, but for a horizontal array. Again, the calculations with constant-$J_c$ agree well with the predictions of analytical models (equation (3)),

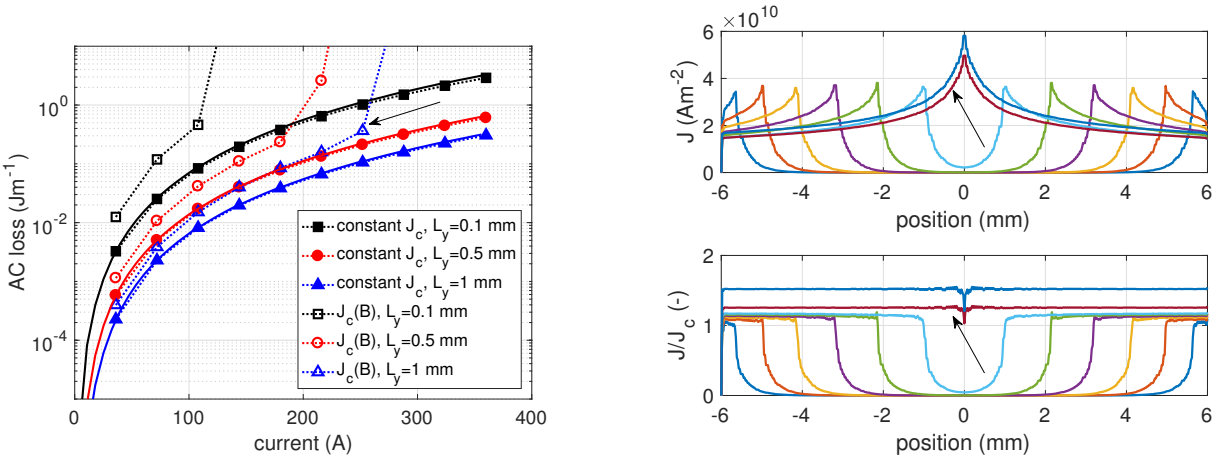


(a) (b)

Figure 7: (a) AC losses of a vertical stack for different separations $L_y$, calculated with constant-$J_c$ (full symbols) and $J_c(B)$ (empty symbols) models, and with equation (4) (continuous lines); b) Current density and normalized current density profiles for $L_y = 1\,\text{mm}$ and $J_c(B)$ for current amplitudes ranging from 36 A to 288 A in steps of 36 A: when $I_0 = 252\,\text{A}$, the superconductor is saturated with current, which leads to a rapid increase of the losses (see arrows in figure 7).

given by the continuous lines. However, in this case, the calculations with $J_c(B)$ differ from those with constant-$J_c$ in the entire current range. In the case of a horizontal array, the magnetic field perpendicular to the flat face of the superconductor is strongly reduced and the current tends to flow only in a very small region close to the edges [22]. With a $J_c(B)$ model, this is also where $J_c$ gets reduced. As can be seen in figure 8b, the dissipative region where $J \geq J_c$ is always very small, even when the transport current is significant. As the transport current increases, the fronts with $J \geq J_c$ do not advance toward the center as in the case of the stack (figure 8b); instead, more current flows in the center of the tape, but $J$ remains subcritical. Hence, contrary to what observed for the stack, the losses do not sharply increase.

## 4. Conclusion

In this article, we used finite-element-method simulations based on the $H$-formulation with constant and magnetic-field-dependent $J_c$ to numerically estimate the AC losses of a thin rectangular superconductor in a variety of scenarios. In the case of a single superconductor subjected to an AC transport current, an AC background field perpendicular to its wide face, or a simultaneous application of current and field, the models gives very similar results, in good agreement with the corresponding analytical models and in reasonably good agreement with experiments. The simulation of infinite stacks and arrays, however, revealed a difference between the two models: in the case of vertical stack with $J_c(B)$, the strong magnetic field generated by the rest of the stack makes the wire easily saturated with current. This saturation occurs at applied currents much lower than the self-field critical current of the single wire. In the case of horizontal arrays, the current always flows in a limited region near the edges. The dissipative area is always limited to that narrow area and the saturation of the tape is avoided. The results obtained with stacks and arrays still need a proper validation against experimental data.

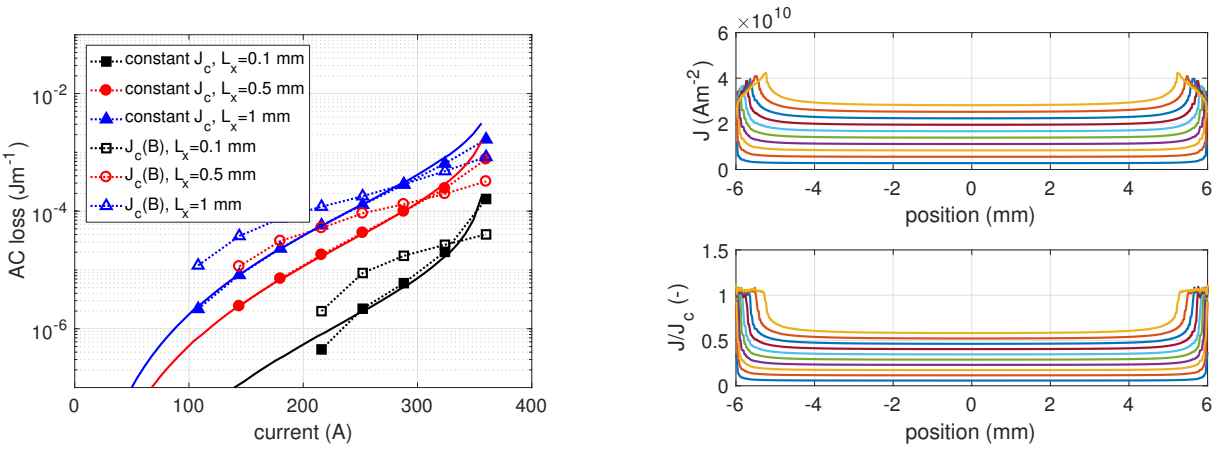


(a) (b)

Figure 8: (a) AC losses of a horizontal array for different separations $L_x$, calculated with constant-$J_c$ (full symbols) and $J_c(B)$ (empty symbols) models, and with equation (3) (continuous lines); b) Current density and normalized current density profiles for $L_x = 1\,\text{mm}$ and $J_c(B)$ for current amplitudes ranging from 36 A to 360 A in steps of 36 A.

## References

[1] Grilli F, Pardo E, Stenvall A, Nguyen D N, Yuan W and Gömöry F 2014 *IEEE Transactions on Applied Superconductivity* **24** 8200433
[2] Bean C P 1962 *Physical Review Letters* **8** 250–252
[3] Bean C P 1964 *Reviews of Modern Physics* **36** 31–39
[4] Campbell A M 2007 *Superconductor Science and Technology* **20** 292–295
[5] Grilli F and Rizzo E 2020 *European Journal of Physics* **41** 045203
[6] Brandt E H and Indenbom M 1993 *Physical Review B* **48** 12893–12906
[7] Zeldov E, Clem J, McElfresh M and Darwin M 1994 *Physical Review B* **49** 9802–9822
[8] Mikitik G P, Mawatari Y, Wan A T S and Sirois F 2013 *IEEE Transactions on Applied Superconductivity* **23** 8001920
[9] Musso A, Breschi M, Ribani P L and Grilli F 2021 *IEEE Transactions on Applied Superconductivity* **31** 5900411
[10] Gömöry F and Klinčok B 2006 *Superconductor Science and Technology* **19** 732–737
[11] Hong Z, Campbell A M and Coombs T A 2006 *Superconductor Science and Technology* **19** 1246–1252
[12] Brambilla R, Grilli F and Martini L 2007 *Superconductor Science and Technology* **20** 16–24
[13] Shen B, Grilli F and Coombs T 2020 *Superconductor Science and Technology* **33** 033002
[14] Shen B, Grilli F and Coombs T 2020 *IEEE Access* **8** 100403–100414
[15] Ogawa J, Nakayama H, Odaka S and Tsukamoto O 2004 *Physica C* **412-414** 1021–1025
[16] Gömöry F, Vojenčiak M, Pardo E, Solovyov M and Šouc J 2010 *Superconductor Science and Technology* **23** 034012
[17] Shen B, Li C, Geng J, Zhang X, Gawith J, Ma J, Liu Y, Grilli F and Coombs T A 2018 *Superconductor Science and Technology* **31** 075005
[18] Marchevsky M, Zhang E, Xie Y, Selvamanickam V and Ganesan P G 2009 *IEEE Transactions on Applied Superconductivity* **19** 3094–3097
[19] Demenčík E, Vojenčiak M, Kario A, Nast R, Jung A, Goldacker W and Grilli F 2014 *IEEE Transactions on Applied Superconductivity* **24** 6601008
[20] Solovyov M, Pardo E, Souc J, Gömöry F, Skarba M, Konopka P, Pekarčíková M and Janovec J 2013 *Superconductor Science and Technology* **26** 115013
[21] Ogawa J, Nakayama H, Odaka S and Tsukamoto O 2005 *Cryogenics* **45** 23–27
[22] K-H Müller 1997 *Physica C* **289** 123–130